Title

Lessons from relatives: C4 photosynthesis enhances CO_2 assimilation during the low-light phase of fluctuations.

Authors

Lucía Arce Cubas[1], Cristina Rodrigues Gabriel Sales[1], Richard L. Vath[1], Emmanuel L. Bernardo[1,2], Angela C. Burnett[1], Johannes Kromdijk[1,3]*

Affiliations

[1]University of Cambridge, Department of Plant Sciences, Downing Street, CB2 3EA Cambridge, United Kingdom.

[2]Institute of Crop Science, College of Agriculture and Food Science, University of the Philippines Los Baños, College, Laguna 4031, Philippines.

[3]Carl R Woese Institute for Genomic Biology, University of Illinois at Urbana-Champaign, 61801 Urbana, Illinois, USA.

***Author for correspondence**

jk417@cam.ac.uk

Running head (max 50 characters)

C_3 versus C_4 photosynthesis under fluctuating light

One sentence significance statement

Comparing photosynthesis in three pairs of closely related C_3 and C_4 species across three fluctuating light regimes showed that C_4 photosynthesis has a systematic advantage under the low light phase not related to suppression of photorespiration, while the comparative efficiency under the high light phase was not determined by photosynthetic pathway.

Abstract

Despite the global importance of species with C_4 photosynthesis, there is a lack of consensus regarding C_4 performance under fluctuating light. Contrasting hypotheses and experimental evidence suggest that C_4 photosynthesis is either less, or more efficient in fixing carbon under fluctuating light than the ancestral C_3 form. Two main issues were identified that may underly the lack of consensus: neglect of evolutionary distance between selected C_3 and C_4 species and use of contrasting fluctuating light treatments. To circumvent these issues, we compared photosynthetic responses to fluctuating light across three independent phylogenetically controlled comparisons between C_3 and C_4 species from *Alloteropsis*, *Flaveria*, and *Cleome* genera under 21% and 2% O_2. Leaves were subjected to repetitive stepwise changes in light intensity (800 and 100 µmol m^{-2} s^{-1} PFD) with three contrasting durations: 6, 30 and 300 seconds. These experiments reconcile the opposing results found across previous studies showing that 1) stimulation of CO_2 assimilation in C_4 species during the low light phase was both stronger and more sustained than in C_3 species; 2) CO_2 assimilation patterns during the high light phase were genus-specific rather than impacted by photosynthetic pathway; and 3) the duration of each light step in the fluctuation regime can strongly influence experimental outcomes.

Introduction

Plants exhibiting C_4 photosynthesis are mostly found in warm, high light environments (Sage, 2000). Although these environments lead to high light intensity at the top of plant canopies, the light conditions experienced by leaves within the canopy can be extremely dynamic. Indeed, sun angle and cloud cover can alter light intensity by orders of magnitude on a second to minute scale, and shading by higher leaves can further modify the temporal fluctuations experienced by individual leaves. Several C_4 species form dense canopies with extensive self-shading where sunflecks can provide up to 90% of the energy for photochemistry (Pearcy, 1990, Slattery et al., 2018, Tang et al., 1988, Way and Pearcy, 2012, Zhu et al., 2004). Since photosynthetic responses to changes in light are not instantaneous, fluctuating light has been identified as an area of improvement for crop productivity (Acevedo-Siaca et al., 2020, Kaiser et al., 2018, Kromdijk et al., 2016, Lawson et al., 2012, Long et al., 2006, Pearcy, 1990, Taylor and Long, 2017). Although recent studies have begun to characterise the C_4 response (Kubásek et al., 2013, Lee et al., 2022, Li et al., 2021, Pignon et al., 2021), most of our understanding of the limitations of photosynthesis under fluctuating light still comes from C_3 species (Kaiser et al., 2018, Pearcy, 1990, Pearcy et al., 1997). Despite the undeniable global importance of C_4 crops, with maize and sugarcane alone accounting for over 30% of global agricultural production (FAO, 2020), the impact of the CO_2 concentrating C_4 acid shuttle on photosynthetic performance in dynamic light remains understudied (Sales et al., 2021, Slattery et al., 2018)

C_4 photosynthesis is a remarkably ubiquitous adaptation that has evolved independently at least 66 times in angiosperms (Kellogg, 2013) and typically leads to faster photosynthetic rates, higher yields, and greater water use efficiency than the ancestral C_3 pathway (Kiniry et al., 1989, Sage, 2004). Most C_4 species operate their carbon concentrating mechanism (CCM) by compartmentalising initial carbon fixation and assimilation between the morphologically distinct mesophyll (M) and bundle sheath (BS) cells, arranged concentrically around the leaf vasculature in 'Kranz' anatomy. In the cytosol of M cells, CO_2 is rapidly converted to bicarbonate by carbonic anhydrase and fixed by phosphoenolpyruvate carboxylase (PEPC) into a 4-carbon oxaloacetate molecule that is further reduced into more stable metabolites malate (Mal) or aspartate (Asp) for transport into the BS. The 4-carbon molecules are decarboxylated in the BS to concentrate CO_2 around the carbon-fixing enzyme ribulose 1,5-biphosphate carboxylase/oxygenase (Rubisco) and thus enhance photosynthesis by suppressing Rubisco's alternative oxygenation reaction and resulting photorespiration, which consumes energy and reducing equivalents and re-releases CO_2 (Leegood, 2002). Reduced carbon in the form of

alanine (Ala) or pyruvate is then transported back to the M cells, where phosphoenolpyruvate (PEP) is regenerated at the cost of ATP, imposing an additional cost to C_4 metabolism. The specific transport metabolites and enzymes of the C_4 pathway vary, and whilst species were traditionally classified based on predominant decarboxylases nicotinamide adenine dinucleotide-malic enzyme (NAD-ME), nicotinamide adenine dinucleotide phosphate-malic enzyme (NADP-ME), and phosphoenolpyruvate carboxykinase (PEPCK) (Hatch et al., 1975), there is a growing consensus that different decarboxylating enzymes often operate in conjunction, with PEPCK likely acting predominantly as a supplementary pathway (Calsa and Figueira, 2007, Furbank, 2011, Pick et al., 2013, Sales et al., 2018). Crucially, intercellular transport of C_4 intermediates is driven by diffusion, making the establishment of high metabolic gradients a requirement for the operation of the CCM (Arrivault et al., 2017, Leegood and Furbank, 1984, Lilley et al., 1977, Stitt et al., 1985), although model simulations suggest mixed C_4 pathways could be less reliant on large metabolite pools (Wang et al., 2012).

Studies conducted on C_3 species show that the response of CO_2 assimilation to fluctuating light is restricted by several factors: slow stomatal opening reduces CO_2 diffusive transfer into the leaf and slow stomatal closing decreases water use efficiency (McAusland et al., 2016), Rubisco activation and the regeneration of ribulose-1,5-biphosphate (RuBP) delay C_3 cycle activity (Mott and Woodrow, 2000, Pearcy and Seemann, 1990, Sassenrath-Cole and Pearcy, 1992), and the speed of up- and down-regulation of photoprotection lowers light use efficiency (Niu et al., 2022, Zhu et al., 2004). Although said limitations exist irrespective of photosynthetic pathway, C_4 species have the additional challenge of coordinating the C_3 and C_4 cycles (Kromdijk et al., 2014), and perhaps due to this additional complexity, the specific C_4 response to fluctuating light is not yet fully understood (Kaiser et al., 2018, Slattery et al., 2018). Two apparently contradictory hypotheses can be found in the literature – where C_4 photosynthesis is suggested to be either less (Kubásek et al., 2013, Li et al. 2021), or more efficient (Stitt and Zhu, 2014) under fluctuating light than the ancestral C_3 form.

The first hypothesis suggests that C_4 species are more negatively impacted by sudden changes in light intensity due to the C_3 and C_4 cycles temporarily operating asynchronously (Sage and McKown, 2006). Fluctuations in light could disrupt the build-up of metabolic gradients necessary for the effective operation of the CCM, leading to impaired suppression of photorespiration and reduced photosynthetic efficiency (Kromdijk et al., 2010, Slattery et al., 2018). Alternatively, if the CCM is faster to activate during light induction than the C_3 cycle

there could be transient over-pumping of CO_2 and an increase in BS leakiness – where CO_2 diffuses out of BS cells back into M cells, raising the energetic cost of carbon fixation due to the futile cycling of PEP. Greater BS leakiness during induction relative to steady state has been previously observed in maize and sorghum (Wang et al., 2022). Lags in CCM deactivation during transitions to lower light could also increase leakiness and reduce quantum yields if Mal/Asp accumulated in the BS is decarboxylated despite insufficient C_3 cycle activity. In further support for the "negative effect" hypothesis, previous studies have found assimilation rates under fluctuating light relative to steady state to be almost four times lower in C_4 compared to C_3 species due to slower photosynthetic induction (Li et al., 2021), as well as a more pronounced reduction of biomass in C_4 than C_3 plants grown under fluctuating compared to steady light conditions (Kubásek et al., 2013).

The second hypothesis instead posits that C_4 species are better able to buffer against sudden changes in light intensity because the large metabolite pools required to drive the CCM can store and release ATP and reducing equivalents (Stitt and Zhu, 2014). The reversible reactions linking the exchange of 3-phosphoglyceric acid (3-PGA) and triose phosphates (TP) between M and BS cells could provide or consume ATP and NADPH to support the C_3 cycle (Leegood and von Caemmerer, 1989); and mixed C_4 pathways could transiently enhance Mal over Asp decarboxylation to temporarily increase transport of redox equivalents into the BS (Wang et al., 2014a). In favour of the "positive effect" hypothesis, some of the highest post-illumination CO_2 fixation rates have been found in C_4 species (Laisk and Edwards, 1997), and a recent study on grasses recorded higher rates of carbon assimilation in C_4 over C_3 species under fluctuating light due to slower decreases in photosynthetic capacity during high-to-low light transitions (Lee et al., 2022).

Although seemingly opposing, there are indications that both hypotheses may coexist. Features of C_4 biochemistry could have mixed effects – the need to establish large metabolite pools could slow photosynthetic induction but enable higher rates of assimilation upon transitioning to a lower light intensity. Slattery et al. (2018) estimated the buffering capacity of C_4 photosynthesis to be limited to 10-15 seconds based on maize metabolite pool sampling (Arrivault et al., 2017) and suggested that the specific C_4 response could thus depend on the length of light fluctuations. A time-sensitive response could account for the different responses observed between sunflecks (Laisk and Edwards, 1997) and longer fluctuations (Kubásek et al., 2013, Li et al., 2021). However, the different light treatments and species used across

studies makes it difficult to draw clear conclusions. This is further complicated by C_4 subtype-specific responses like the post-illumination CO_2 burst often observed in NADP-ME species (Krall and Pearcy, 1993, Lee et al., 2022), as well as lack of consideration of phylogenetic distance, which can strongly confound comparisons between photosynthetic pathways (Taylor et al., 2010), leading to the inappropriate association of species-specific phenomena with the presence or absence of the C_4 pathway.

In this study, we compared the photosynthetic response to fluctuating light in relation to steady state across three phylogenetically linked pairs of C_3 and C_4 species from *Alloteropsis* (C_3 *Alloteropsis semialata GMT* & C_4 *Alloteropsis semialata MDG*), *Flaveria* (C_3 *Flaveria cronquistii* & C_4 *Flaveria bidentis*), and *Cleome* (C_3 *Tarenaya hassleriana* & C_4 *Gynandropsis gynandra*) genera. Together, these three pairs contain both monocots and dicots, and all three C_4 decarboxylase subgroups. To compare gas exchange responses across the three pairs, fluctuating light treatments consisting of repetitive stepwise changes in light intensity from 800 to 100 µmol m^{-2} s^{-1} photon flux density (PFD) were used, with three different light step durations: 6, 30, and 300 seconds. To evaluate the impact of photorespiration on the responses to fluctuating light, experiments were conducted under both 2% and 21% oxygen concentration. We hypothesised that 1) after a transition to low light, C_4 species will be better able to sustain photosynthetic rates than C_3 species, even when photorespiration is suppressed, 2) C_4 species will incur a higher penalty during transitions to high light; and 3) the impact of both effects will be inversely correlated to fluctuation length.

Results

Steady state responses of CO_2 assimilation in paired C_3 and C_4 species are consistent with well-established differences between photosynthetic pathways.

To provide a baseline for comparing CO_2 assimilation rates between three pairs of closely related C_3 and C_4 species under fluctuating light, first the steady state light response of photosynthetic gas exchange was measured under 21% and 2% O_2 to minimize photorespiration (**Figure 1**). We focus here on photosynthetic parameters at the light intensities that were used in subsequent fluctuating light treatments, 800 and 100 µmol m^{-2} s^{-1} PFD (**Table 1**). Two-way ANOVA was used to assess the effects of photosynthetic pathway, oxygen concentration, and their interactions within each genus (**Table 2**). At both light intensities C_3 species trended towards higher assimilation values and quantum yields under photorespiration-suppressing (2% O_2) conditions than C_4 species.

At 800 µmol m^{-2} s^{-1} PFD, net CO_2 assimilation (A_{CO2}) values in C_4 *A. semialata MDG* (12.3 ± 0.5 µmol m^{-2} s^{-1}), C_4 *F. bidentis* (18.7 ± 1.0 µmol m^{-2} s^{-1}), and C_4 *G. gynandra* (23.5 ± 2.0 µmol m^{-2} s^{-1}) were respectively higher than phylogenetic pairs C_3 *A. semialata GMT* (11.3 ± 0.9 µmol m^{-2} s^{-1}), C_3 *F. cronquistii* (13.8 ± 1.4 µmol m^{-2} s^{-1}), and C_3 *T. hassleriana* (14.6 ± 0.5 µmol m^{-2} s^{-1}). Under 2% oxygen, photosynthetic rates increased by 33% in C_3 *A. semialata GMT*, 81% in C_3 *F. cronquistii,* and 86% in C_3 *T. hassleriana*, compared to a more modest increase of 6%, 15% and 16% in their respective C_4 pairs, leading to significant effects of O_2 at 800 µmol m^{-2} s^{-1} PFD on A_{CO2} as well as on quantum yield of CO_2 assimilation (ΦCO_2) across all three genera ($p \leq 0.02$).

At 100 µmol m^{-2} s^{-1} PFD, the effects of photosynthetic pathway, O_2 concentration and their interaction on A_{CO2} varied between genera. In *Alloteropsis,* none of the effects were significant, although C_4 *A. semialata MDG* (4.7 ± 0.5 µmol m^{-2} s^{-1}) showed slightly higher A_{CO2} values than C_3 *A. semialata GMT* (3.2 ± 0.5 µmol m^{-2} s^{-1}) under ambient O_2. In *Flaveria,* values of A_{CO2} were similar under ambient O_2 in C_4 *F. bidentis* (4.2 ± 0.3 µmol m^{-2} s^{-1}), and C_3 *F. cronquistii* (3.9 ± 0.2 µmol m^{-2} s^{-1}), but significantly higher in C_3 *F. cronquistii* under 2% O_2 (4.7 ± 0.4 vs 6.6 ± 0.3 µmol m^{-2} s^{-1}, respectively). As a result, both the main effects of O_2 and photosynthetic pathway as well as their interaction on both A_{CO2} and ΦCO_2 were significant in *Flaveria* ($p \leq 0.02$). In *Cleome*, A_{CO2} under 21% O_2 was lower in C_4 *G. gynandra* (3.2 ± 0.4 µmol m^{-2} s^{-1}) than in C_3 *T. hassleriana* (4.1 ± 0.2 µmol m^{-2} s^{-1}) and both rates increased under 2% O_2 (4.7 ± 0.5 and 6.2 ± 0.6 µmol m^{-2} s^{-1}, respectively), resulting in significant effects of both photosynthetic pathway and O_2 concentration ($p \leq 0.02$).

CO_2 assimilation under fluctuating light differs between genera and is significantly affected by fluctuation frequency, photosynthetic pathway, and oxygen concentration

After characterising steady state light responses, CO_2 assimilation rates were measured in response to three different 1-hour fluctuating light treatments. Each treatment consisted of acclimation at 150 µmol m^{-2} s^{-1} PFD, followed by repetitive stepwise changes between 800 and 100 µmol m^{-2} s^{-1} PFD where each light step lasted 6, 30, or 300 seconds. Data from minutes 50-60 of each treatment (**Figure 2**) were used for analysis to exclude the effect of initial induction (for the complete timeseries see **Supplementary figure 1**). The fluctuating light response generally consisted of a rise in A_{CO2} towards steady state in the 800 µmol m^{-2} s^{-1} PFD period, and a subsequent decrease during the 100 µmol m^{-2} s^{-1} PFD period. A_{CO2} was strongly increased under 2% O_2 in the C_3 species, but much less so in the C_4 species. More subtle patterns varied by photosynthetic type, fluctuation length, and between genera as described below.

After transitioning from 800 to 100 µmol m^{-2} s^{-1} PFD, A_{CO2} in C_4 *A. semialata MDG* and C_4 *F. bidentis* decreased more gradually compared to the immediate drop followed by a gradual rise towards steady state observed in C_3 *A. semialata GMT,* C_3 *F. cronquistii* and C_3 *T. hassleriana*. This instantaneous drop in assimilation in the C_3 species at the start of the 100 µmol m^{-2} s^{-1} PFD period is commonly attributed to photorespiration (Forrester et al., 1966, Wynn et al., 1973), and indeed was suppressed in all C_3 species under 2% oxygen (most easily seen in **Figure 2 C/F/I** compared to **Figure 2 L/O/R)**. The slower decrease of A_{CO2} in C_4 *A. semialata MDG* and C_4 *F. bidentis* was evident under 30 s (**Figure 2 B/E**) and 300 s light steps (**Figure 2 C/F**) in both oxygen concentrations, whilst under 6 s light steps (**Figure 2 A/D**) A_{CO2} at 100 µmol m^{-2} s^{-1} stayed closer to rates obtained during the 800 µmol m^{-2} s^{-1} PFD periods, suggesting a less significant initial decline. Irrespective of oxygen concentration and unlike the delayed decrease observed in the other C_4 species, in C_4 *G. gynandra* an initial dip in A_{CO2} was observed immediately following the transition to low light (**Figure 2 I/R**).

Following the transition from 100 to 800 µmol m^{-2} s^{-1} PFD, induction patterns strongly varied between the three C_4 species, in contrast with the more consistent patterns observed in C_3 species. C_4 *F. bidentis* and C_4 *G. gynandra* had higher A_{CO2} during the 300 s light steps than C_3 *F. bidentis* and C_3 *T. hassleriana* (**Figure 2 C/F**), but similar or lower A_{CO2} than their C_3 counterparts during the 30 s light step (**Figure 2 B/E**) even under 21% oxygen, suggesting a comparatively greater lag in photosynthetic induction. However, induction of A_{CO2} in C_4 *A. semialata MDG* was very similar to that of C_3 *A. semialata GMT*. In C_4 *G. gynandra* a strong

temporary depression in A_{CO2} was observed after an initial sharp increase upon exposure to higher light under the 300 s light step that was not affected by the suppression of photorespiration by low oxygen (see **Figure 2 I vs R**).

To compare photosynthetic performance between C_3 and C_4 species whilst accounting for their different steady state photosynthetic capacities, A_{CO2} was expressed as a relative percentage of steady state values obtained from light response curves (percentages across a single fluctuation are shown in **Figure 3**. For the corresponding carbon assimilation values see **Supplementary figure 2**, which were compared to the steady state values in **Table 2/Figure 1**). This analysis showed clear, systematic differences between C_3 and C_4 species during the 100 µmol m^{-2} s^{-1} PFD steps, where all C_4 species were able to sustain higher A_{CO2} under 100 µmol m^{-2} s^{-1} relative to steady state than their matching C_3 counterparts under both 21% and 2% oxygen. However, no clear trend between photosynthetic types was apparent during the 800 µmol m^{-2} s^{-1} PFD steps.

Stimulation of CO_2 assimilation at low light phase of fluctuations is most prominent in short light steps and significantly greater in C_4 compared to C_3 species.

To quantify the stimulation of A_{CO2} during the 100 µmol m^{-2} s^{-1} PFD steps of the fluctuations, the average A_{CO2} during the 100 µmol m^{-2} s^{-1} PFD steps was normalized against the steady state rate at the same intensity (**Figure 4 D-F**, for a boxplot of the absolute A_{CO2} values see **Supplementary figure 3 E-G**). This analysis showed that assimilation was higher than steady state (as seen in the **Figure 3** grey half, values greater than 100%) in all species immediately following the transition but declined with duration of the light steps (**Table 3**, $p \leq 0.001$ for all). In addition, the relative stimulation compared to steady state values was consistently significantly greater in the C_4 species compared to the C_3 species in the *Flaveria* and *Cleome* pairs (*Flaveria* $p \leq 0.01$; *Cleome* $p \leq 0.001$). Although not significant, a similar trend was observed for the *Alloteropsis* pair at 300 s and 30 s, but not at 6 s light steps.

Three-way ANOVA (**Table 3**) showed A_{CO2} relative to steady state was significantly affected by fluctuation length in all genera ($p \leq 0.001$ for all), as well as by photosynthetic pathway in *Flaveria* and *Cleome* (*Flaveria* $p \leq 0.01$; *Cleome* $p \leq 0.001$). Overall, although all species had greater CO_2 fixation during the 100 µmol m^{-2} s^{-1} PFD periods than under steady state, the effect was time sensitive and therefore more significant during shorter light steps. In addition, C_4 species were able to sustain the higher rates for longer than their C_3 counterparts. The greatest increases in relative assimilation occurred during the 6 s light steps (**Figure 4 D**) where C_4 species were on average 329% of steady state A_{CO2} compared to 242% in C_3 species under 21%

oxygen and similarly 290% in C_4 vs 243% in C_3 at 2% oxygen. Under 30 s light steps (**Figure 4 E**) the stimulation of A_{CO2} relative to steady state was less pronounced than 6 s, but still significantly higher in C_4 species at 187% compared to C_3 species at 114% of steady state A_{CO2} at 21% O_2, and 190% vs 146% of steady state A_{CO2} at 2% O_2, respectively. The impact of C_4 photosynthesis was most apparent under these two light steps, whereas during the 300 s light steps (**Figure 4 F**) the stimulation of A_{CO2} was generally less evident. Averaged across the 300 s, C_4 species were operating at 132% relative to steady state A_{CO2} compared to C_3 species at 103% under ambient oxygen, and at 130% and 109% of steady state A_{CO2} under 2% O_2, respectively. Interestingly, A_{CO2} relative to steady state across all three light step durations was typically higher in C_4 compared to C_3 species under both 21% and 2% oxygen and no significant effect of the interaction between photosynthetic pathway and oxygen concentration was found in any of the genera, suggesting a systematic advantage to C_4 photosynthesis to bridge low light periods which was not explained by suppression of photorespiration.

To estimate to what extent the low light stimulation of CO_2 assimilation was decoupled from photochemical provision of ATP and NADPH, ΦCO_2 was calculated for each light step (**Figure 5, Table 4**). Based on steady state stoichiometry of electron flow and proton requirements for ATP synthesis and NADPH:ATP energy demands, the theoretical maximum ΦCO_2 has been estimated as 0.111 CO_2/photon for C_3 species (Ehleringer and Pearcy, 1983), as 0.064 CO_2/photon for C_4 NADP-ME and NAD-ME species accounting for BS leakiness (Yin and Struik, 2018), and due to the theorised lower energy requirements of mixed C_4 pathways as 0.075 CO_2/photon for mixed subtype NADP-ME-PEPCK (Ishikawa et al., 2016, Yin and Struik, 2021). Here we consider observations of quantum yields exceeding these theoretical maxima as conservative estimates for the degree of decoupling. At 6 s light steps, C_3 *F. cronquistii* and C_3 *A. semialata GMT* stayed well below the theoretical maximum, but the ΦCO_2 values of C_3 *T. hassleriana* were significantly higher. ΦCO_2 values of C_4 *A. semialata MDG,* C_4 *F. bidentis, and* C_4 *G. gynandra* during the lower light periods of the 6 s and 30 s fluctuations were also significantly higher than the theoretical limit, suggesting that the provision of ATP and reductant was not directly coupled to production from the thylakoid reactions. By comparing the ΦCO_2 values with these theoretical maxima, it is possible to estimate the degree of decoupling in units of fixed CO_2/photon. At 6 s light steps, the theoretical limit was exceeded by 0.043 ± 0.019 CO_2/photon in C_4 *A. semialata MDG*, 0.022 ± 0.008 CO_2/photon in C_4 *F. bidentis,* 0.091 ± 0.008 CO_2/photon in C_4 *G. gynandra* and 0.042 ± 0.008 CO_2/photon in C_3 *T. hassleriana*. At 30 s light steps, these numbers decreased to 0.021 ± 0.011

CO_2/photon in C_4 *A. semialata MDG*; 0.008 ± 0.005 CO_2/photon in C_4 *F. bidentis*; and 0.005 ± 0.003 CO_2/photon in C_4 *G. gynandra*.

Depression of CO_2 assimilation at high light phase of fluctuations is not significantly affected by photosynthetic pathway

Unlike in the 100 µmol m^{-2} s^{-1} PFD periods there was no clear trend between the C_3 and C_4 response at 800 µmol m^{-2} s^{-1} PFD periods (**Figure 4 A-C**, for a boxplot of the corresponding A_{CO2} values see **Supplementary figure 3 A-C**).

A_{CO2} values during the 800 µmol m^{-2} s^{-1} PFD light steps were lower than under steady state (below 100% line in **Figure 3**). Three-way ANOVA (**Table 3**) was used to analyse the effects of light step duration, photosynthetic pathway, oxygen concentration, and their interactions on relative A_{CO2}. None of these were significant for the *Alloteropsis* subspecies. In *Flaveria*, weakly significant interactions between light step duration and photosynthetic pathway (p = 0.04), as well as between oxygen concentration and photosynthetic pathway (p = 0.04) were observed, indicating a more complex conditional impact of photosynthetic pathway on assimilation rate relative to steady state. In C_4 *F. bidentis* relative A_{CO2} gradually increased with light step duration, whereas in C_3 *F. cronquistii* this increase was only observed between 6 and 30 s but had reached a plateau between 30 and 300 s. Whilst relative A_{CO2} was depressed by 2% oxygen in both *Flaveria* species, the effect was more pronounced in C_3 *F. cronquistii*. In *Cleome*, light step duration significantly impacted relative A_{CO2} (p = 0.01) which increased with duration in both C_3 and C_4 species.

Quantum yields during the 800 µmol m^{-2} s^{-1} PFD periods across all fluctuation regimes and oxygen concentrations were lower than steady state across all species (**Figure 5 A-D**), indicating reduced efficiency of carbon assimilation. In *Alloteropsis*, oxygen concentration significantly impacted ΦCO_2 (p = 0.01, **Table 4**), with 2% oxygen being associated with higher values. In *Flaveria* and *Cleome* 2% oxygen was associated with higher quantum yields only in the C_3 species, and lower or similar values in their C_4 counterparts (significant interactions between O_2 and photosynthetic pathway $p \leq 0.05$).

Discussion

C_4 species are better able to sustain photosynthetic rates than C_3 species during the low light phase of fluctuations

The effect of fluctuating light on C_4 relative to C_3 photosynthesis was systematically evaluated in three phylogenetically controlled comparisons using repetitive low and high light steps with three contrasting durations. The results support the hypothesis that C_4 species are better able to sustain photosynthetic rates than C_3 species during the lower light periods of fluctuating light. The theoretical basis for this hypothesis suggests that the large metabolite pools necessary for diffusional transfer between M and BS in C_4 photosynthesis and the reversible reactions linking these metabolic intermediates can work as a capacitor, providing greater flexibility to respond to variations in light intensity (Leegood and von Caemmerer, 1989, Stitt and Zhu, 2014). In this study, although all tested species had generally higher carbon assimilation during the 100 µmol m^{-2} s^{-1} PFD periods relative to steady state, C_4 *A. semialata MDG,* C_4 *F. bidentis*, and C_4 *G. gynandra* were elevated higher above steady state than C_3 *A. semialata GMT*, C_3 *F. bidentis,* and C_3 *T. hassleriana* under the same fluctuating light regime (**Figure 4 D-F**). As C_4 species had higher relative assimilation under both 21% and 2% oxygen, the greater stimulation under low light cannot be solely attributed to increased presence of photorespiration in C_3 species during fluctuating light, and the prevalence of this result across species from diverse evolutionary lineages and C_4 subtypes suggests that this ability to sustain high photosynthetic rates after a transition to lower light may indeed be linked to other general features of the C_4 pathway – such as the large metabolite pools intrinsic to CCM operation (Arrivault et al., 2017, Leegood and Furbank, 1984, Lilley et al., 1977, Stitt et al., 1985).

Metabolic pools also play a role in C_3 species, and post-illumination CO_2 fixation has previously been attributed to pools of C_3 intermediates, and ATP and redox equivalents that accumulate during higher light fluctuations (Kaiser et al., 2015). In C_3 *A. semialata GMT*, C_3 *F. bidentis,* and C_3 *T. hassleriana*, the higher A_{CO2} values relative to steady state observed during 6 s fluctuations, as well as during the first half of the 30 s fluctuations (**Figure 3 BEH & KNQ**) are in line with previous observations of carbon assimilation exceeding steady state rates immediately after sunflecks (Pons and Pearcy, 1992, Sharkey et al., 1986). However, metabolic pools in C_3 species are typically considerably smaller than in C_4 species (Borghi et al., 2022), which may be why C_4 *A. semialata MDG,* C_4 *F. bidentis*, and C_4 *G. gynandra* were able to sustain higher relative rates for longer than their C_3 counterparts (**Figure 3**), as evidenced by the higher average rates across longer fluctuations (**Figure 4 D-F**). However, the capacity of C_4 species to buffer through transitions to lower light still decreases across time as

metabolite pools are depleted (Slattery et al., 2018), and carbon assimilation relative to steady state during those periods was inversely related to the length of the fluctuations. Altogether, the higher and more sustained stimulation of C_4 photosynthetic rates compared to C_3 rates at low light is consistent with prior work (Laisk and Edwards, 1997, Lee et al., 2022, Li et al., 2021) and explains why studies using different fluctuating light regimes can yield contrasting estimates for the comparative advantage of C_4 versus C_3 photosynthesis.

Finally, the quantum yield of photosynthesis provides another indication of the storage capacity of C_4 metabolic pools. In C_4 species ΦCO_2 during the 6 s and 30 s fluctuations was consistently above the theoretical maximum (Ehleringer and Pearcy, 1983, Ishikawa et al., 2016, Morales et al., 2018, Yin and Struik, 2018, Yin and Struik, 2021), indicating that the energetic equivalent of fixing ~0.022-0.091 CO_2/photon under 6 s fluctuations and ~0.005-0.021 CO_2/photon under 30 s fluctuations was being supplied outside of the thylakoid light reactions. These numbers provide a conservative estimate of the extent of decoupled CO_2 fixation in C_4 species, which may have been sustained by redox equivalents from malate decarboxylation, with demands for ATP and NADH being buffered through reversible reactions linking 3-PGA and TP, or interconversion of 3-PGA and PEP (Arrivault et al., 2017, Bräutigam et al., 2008, Slattery et al., 2018, Stitt and Zhu, 2014, Wang et al., 2014b). Leaf-level and canopy simulations emphasise ΦCO_2 as the largest determinant of photosynthesis in the lower canopy (Bellasio and Farquhar, 2019, Gu et al., 2014) and the stimulation of low light ΦCO_2 as observed here at three contrasting fluctuation frequencies could provide an important mitigation mechanism of the intrinsically lower maximum quantum yield of C_4 plants under low light (Medeiros et al., 2022, Ubierna et al., 2011).

The C_4 response during the transition to higher light is related to the specific subtype metabolism

The comparative high light performance of C_4 photosynthesis was not uniform across the three genera, and instead was impacted by the specific characteristics of the C_4 pathway within each genus. Light fluctuations have been suggested to hinder the formation of the large metabolite pools necessary for optimal CCM operation, resulting in impaired suppression of photorespiration and lagging photosynthetic induction during metabolite build-up (Sage and McKown, 2006). Indeed, we previously found that the C_4 species analysed here were all slower to induce photosynthesis from darkness relative to their C_3 counterparts (Arce Cubas et al., 2023). However, theoretical work indicates that not all subtypes are equally reliant on gradients: mixed C_4 pathways like NADP-ME-PEPCK do not need metabolite gradients as large as

NADP-ME or NAD-ME subtypes, as mixed subtypes can concurrently use different transfer acids (Wang et al., 2014a). The use of both Mal and Asp shuttles also allows for finer regulation of the ATP:NADPH ratio in response to changes in light, as only Mal transport brings redox equivalents into the BS (Yin and Struik, 2021). Consistent with this interpretation, the highest A_{CO2} relative to steady state rates in C_4 species during the 800 µmol m^{-2} s^{-1} PFD periods were found in C_4 *A. semialata MDG* which is suggested to rely on a mixed NADP-ME-PEPCK C_4 pathway (Ueno and Sentoku, 2006) (**Figure 4 A-C**). The lack of effect of light step duration on A_{CO2} during the high light periods in *Alloteropsis* (**Table 3**) can be explained by photosynthetic induction during these fluctuating light regimes being relatively fast (**Figure 2 ABC**). In contrast, high light A_{CO2} relative to steady state was significantly lower with shorter fluctuations in both *Cleome* species; whereas in *Flaveria,* C_4 *F. bidentis* relative assimilation was more significantly reduced during shorter fluctuations than in C_3 *F. cronquistii*, indicating the C_4 cycle lagged behind C_3 activation.

The genus-specific rather than photosynthetic pathway effects detailed above in combination with the varying impact of light step duration provides an important consideration for interpretation of previous work. Li et al. (2021) compared a selection of six C_4 species with eight C_3 species, concluding that C_4 species utilized fluctuating light less efficiently. Our results suggest the slow induction observed in that study could be associated with the selected C_4 species being mostly of the NADP-ME subtype (five out of six, one of which was *F. bidentis*) and one NAD-ME subtype. Indeed, Lee et al. (2022) recently reported distinct species-specific induction patterns across six C_4 grass species. Interestingly, Lee et al. concluded that their selection of C_4 species assimilated more carbon under fluctuating light in comparison with six C_3 species. Aside from the inclusion of different species in both papers, these seemingly opposite conclusions could also be due to a slight difference in fluctuating light treatments. Although both experiments had low light steps of two minutes, high light steps were two minutes in the Li et al. (2021) study and four minutes in Lee et al. (2022). Since both studies observed a slower decrease in photosynthetic rates in C_4 species after the transition to lower light, the additional two minutes of higher light in the Lee et al. study may have reduced the comparative penalty of C_4 induction relative to the benefits of higher assimilation during the lower light periods, explaining the contrasting conclusions.

Fluctuations in light cause CO_2 bursts in C_4 G. gynandra

C_4 *G. gynandra* had distinctive assimilation kinetics after each light transition in the 300 s fluctuations (**Figure 2 I&R**). At the start of the 800 µmol m^{-2} s^{-1} PFD period, a rapid increase in $A_{CO2,}$ described in previous work as a CO_2 gulp (Laisk and Edwards, 1997), was immediately followed by a CO_2 burst, with another CO_2 burst upon changing to the 100 µmol m^{-2} s^{-1} PFD period. These bursts were not a product of photorespiration, as unlike the CO_2 bursts observed after a transition to lower light in C_3 species, in C_4 *G. gynandra* they occurred independent of oxygen concentration.

Previous studies on sunflecks (Laisk and Edwards, 1997) have characterised the post-illumination CO_2 burst as a specific feature of the NAD-ME and PEPCK pathways, and other fluctuating light studies have also reported it primarily for NAD-ME species (Lee et al., 2022). Unlike NADP-ME species, where malate decarboxylation is linked to reducing equivalents from the C_3 cycle, in NAD-ME species the C_3 and C_4 cycles are less tightly coupled – oxaloacetate is first reduced to malate and then decarboxylated in the mitochondria, but the redox balance is uncoupled from the C_3 cycle (Ishikawa et al., 2016). This can result in excess CO_2 being released despite insufficient RuBP regeneration upon a transition to lower light, causing unfixed CO_2 to leak out of the BS and A_{CO2} to drop.

The CO_2 gulp and burst at the start of the 800 µmol m^{-2} s^{-1} PFD period is similar to induction kinetics observed in short dark-light fluctuations in NAD-ME *Amaranthus cruentus* (Laisk and Edwards, 1997). These were attributed to formation of alanine from the decarboxylation of aspartate in low light (or darkness), leading to rapid conversion of alanine to pyruvate followed by phosphorylation to PEP when light is increased (Laisk and Edwards, 1997, Lee et al., 2022). Based on this interpretation. the initial PEP carboxylation following the increase in light would exceed the rate at which PEP pools can be replenished, but subsequently crashes and readjusts while PEP regeneration is re-established. This may account for the observed temporary gulp and subsequent steady increase in A_{CO2}. Furthermore, the centripetal chloroplast positioning found in NAD-ME species (Yoshimura et al., 2004) could increase path length for metabolites and CO_2, and lead to a more pronounced form of the biphasic induction previously observed in NADP-ME species (Lee et al., 2022).

Conclusions

The presented work compared C_4 to C_3 photosynthesis in response to fluctuating light. By using three independent phylogenetically controlled comparisons and fluctuations with three contrasting light step durations the presented work circumvented issues in previous studies to yield more robust conclusions. The results showed that the stimulation of A_{CO2} in the low light phase was both higher and more sustained in C_4 photosynthesis across all three comparisons, suggesting this could be a common comparative advantage of C_4 photosynthesis. In contrast, observed patterns of A_{CO2} in the high light phase were found to be largely genus-specific, rather than attributable to photosynthetic pathway.

Materials and methods

Plant materials

To control for evolutionary distance, three pairs of phylogenetically linked *Alloteropsis*, *Flaveria*, and *Cleome* C_3 and C_4 species (shown in **Table 5**, see also Arce Cubas et al., 2023) were selected. Significant evolutionary distance exists between the selected genera and C_4 photosynthesis evolved independently in each. The C_4 origin dates back approximately 17 million years (Ma) in *Cleome*, ~ 2 Ma in *Flaveria*, and is even more recent in *Alloteropsis* (Christin et al., 2011, Lundgren et al., 2015). In addition, the selected species include both monocots (*Alloteropsis*) and dicots (*Flaveria* and *Cleome*), and all three major decarboxylase enzymes of the C_4 pathway: NADP-ME-PEPCK (C_4 *A. semialata MDG*), NAD-ME (C_4 *F. bidentis*), and NAD-ME (C_4 *G. gynandra*) (Bräutigam et al., 2008, Gowik et al., 2011, Ueno and Sentoku, 2006).

Plant growth and propagation

Flaveria and *Cleome* species were grown in a Conviron walk-in growth room (Conviron Ltd., Winnipeg, MB, CA) at 20 ºC, 60% relative humidity (RH), and 150 µmol m^{-2} s^{-1} PFD over a 16-hour photoperiod; and the *Alloteropsis* accessions in a glasshouse in Cambridge, England, at 18-25 ºC, 40-60% RH, with supplemental lightning to provide a minimum of 140-160 µmol m^{-2} s^{-1} PFD in addition to incoming irradiance. All plants were well-watered and grown in Levington Advance M3 compost (Scotts, Ipswich, UK) mixed with Miracle-Gro All Purpose Continuous Release Osmocote (Scotts Miracle-Gro Company, Marysville, OH, USA; 4 L compost : 25 g Osmocote), with vermiculite being added to the *Alloteropsis* soil mix to prevent waterlogging (1 L vermiculite : 4 L compost : 25 g Osmocote).

Alloteropsis and *Flaveria* species were vegetatively propagated whilst *Cleome* species were grown from seed. *Alloteropsis* MDG and GMT accession tillers were grown in 2 L pots and all gas exchange measurements taken after 2 weeks. For *Flaveria* propagation, lateral shoot cuttings were dipped in Doff Hormone Rooting Powder (Doff Portland Ltd., Hucknall, UK) to induce root development, grown on 0.25 L pots, and measured after 8-10 weeks. *F. cronquistii* requires vegetative propagation, so *F. bidentis* plants were first grown from seed and subsequently propagated via cuttings. *Cleome* germination was induced with a 30 ºC/20 ºC day/night cycle for *T. hassleriana*, and at 30 ºC for *G. gynandra*. The germinated seeds were sown in 24-cell trays before transfer to 0.25 L pots. Due to the different developmental rates of the *Cleome* species, germination was staggered so both species could be measured at approximately the same developmental stage, after 8-10 weeks for *G. gynandra* and 4-6 weeks for *T. hassleriana*. All plants were measured during vegetative state.

Gas exchange measurements at 21% and 2% O_2

Gas exchange under steady and fluctuating light conditions was measured on young, fully expanded leaves using an open gas exchange system (LI-6800, LI-COR, Lincoln, NE, USA) with a Multiphase Flash Fluorometer (MPF) chamber (6800-01A, LI-COR). Chamber conditions were controlled at 410 ppm sample CO_2 concentration, 60% relative humidity with average leaf VPD of 1.3 ± 0.1 kPa, 25 ºC heat exchanger temperature, and flow rate of 600 µmol s^{-1}. Actinic light was provided by the MPF and composed of 90% red (625 nm) and 10% blue light (475 nm).

For experiments in 2% O_2, a pre-mixed 2% O_2 and 98% N_2 gas mixture (BOC Ltd., Woking, UK) was supplied to the LI-6800 through the air inlet using a mass flow controller (EL-FLOW, Bronkhorst Hight-tech BV, Ruurlo, NL) and an open T-junction to regulate constant surplus flow according to manufacturer instructions. The LI-6800 Infrared Gas Analyser (IRGA) calibration was adjusted to the O_2 concentration in the instrument constants prior to measurement.

Steady state light response curves

Photosynthetic responses to steady light were measured for all species at both 21% and 2% O_2. Leaves were illuminated with 1000 µmol m^{-2} s^{-1} PFD for 20-40 minutes to allow CO_2 assimilation and stomatal conductance to reach steady state, and gas exchange was subsequently measured in a descending gradient of light intensity: 2000, 1700, 1500, 1200, 1000, 800, 600, 400, 300, 200, 100, 75, 30 and 0 µmol m^{-2} s^{-1} PFD. Gas exchange parameters were logged between 120 – 240 seconds at a given light intensity, when leaf intracellular CO_2 concentration (C_i) and CO_2 assimilation were stable.

Respiration in the light (*Rd*) was estimated from the y-intercept of a linear regression of the slope before the inflection point. Measurements at 0 and 30 µmol m^{-2} s^{-1} PFD were not included in the regression to account for the Kok effect (Kok, 1949). Photosynthetic rates and C_i at 100 and 800 µmol m^{-2} s^{-1} PFD were taken as the steady state values for comparison with fluctuating light measurements. ΦCO_2 was calculated using **Equation 1**.

$$\phi CO_2 = \frac{A_{CO2} + Rd}{PFD_{abs}} \quad \textbf{Equation 1}$$

Fluctuating light experiments and analysis

To measure photosynthetic responses to fluctuating light, leaves were first acclimated at 150 µmol m^{-2} s^{-1} PFD for 30-60 minutes until stomatal conductance and photosynthetic rates reached constant levels. Using a custom program, leaves were then exposed to repetitive stepwise fluctuations in light intensity from 800 to 100 µmol m^{-2} s^{-1} PFD for 1 hour, with gas exchange parameters recorded every 2 seconds. Three different light treatments were tested, with each light step lasting 6, 30, or 300 seconds. To avoid interference with the shorter fluctuations and the data sampling interval the averaging time of the LI-6800 was set to zero, as was additional averaging time, and the IRGAs were only matched prior to the program starting. All fluctuating light treatments were conducted at both 21% and 2% O_2.

As measurements during light fluctuations violate the steady state assumption underlying default rate equations, a storage flux term for CO_2 and H_2O was computed from changes in cuvette concentration between timepoints and applied to adjust carbon assimilation and transpiration rates – and consequently to other instrument calculations derived from those values – using **Equation 2 and 3**.

$$\boldsymbol{Storage}\ flux_{H2O} = \frac{\Delta mole_{H2O}}{S\ x\ t} \quad \textbf{Equation 2}$$

$$\boldsymbol{Storage}\ flux_{CO2} = \frac{-\Delta mole_{CO2}}{S\ x\ t} \quad \textbf{Equation 3}$$

The Δ change in moles of CO_2 or H_2O was calculated from the cuvette volume $8.67e^{-5}$ m^3 using the ideal gas law with instrument recordings of current and previous gas concentration, pressure, and air temperature, and converted to storage flux with leaf area (S) and time since last log (t). The signum reconciles CO_2 flux with the consensus of uptake flux being positive.

Leaf absorptance

After gas exchange measurements, the spectral qualities of the leaves were measured with an integrating sphere (LI-1800-12, LI-COR) optically connected to a miniature spectrometer (STS-VIS, Ocean Insight, Orlando, FL, USA) following manufacturer instructions (LI-COR, 1988). Leaf absorptance (L_{abs}) was calculated using **Equation 4**, where T_s and R_s are transmittance and reflectance of a diffuse sample.

$$L_{abs} = 1 - T_s - R_s \quad \textbf{Equation 4}$$

For the light response curves, incident PFD was converted to absorbed PFD (PFD_{abs}) using L_{abs} of the red and blue emission wavelengths of the 6800-01A MPF light source. For the specific absorptance values, see **Supplementary table 1**.

Data processing

Data from the last 10 minutes of the fluctuating light treatment were used for further analysis. To analyse the relative performance of each species, net photosynthesis (A_{CO2}) under fluctuating light was expressed as a percentage of the steady state rates achieved at the corresponding light intensity. Additionally, ΦCO_2 under fluctuating light was calculated using **Equation 1**.

The area under the curve (AUC) (Makowski et al., 2019) of A_{CO2} relative to steady state and ΦCO_2 during the 100 and 800 µmol m^{-2} s^{-1} PFD periods of the light treatment was integrated using the trapezoidal rule (Jawień, 2014) and divided by the duration to obtain an average value for each light level which was used to compare between fluctuations of different length and, in the case of ΦCO_2, directly to steady state values.

Statistical analysis

Each phylogenetically controlled comparison was run as an independent experiment, thus statistical analyses were conducted separately on paired *Alloteropsis*, *Flaveria,* and *Cleome* light response curves (*800* A_{CO2}, *100* A_{CO2}, $C_{i\ 800}$, $C_{i\ 100}$, *800* ΦCO_2, *100* ΦCO_2, *Rd*), and fluctuating light measurements (A_{CO2} relative to steady state, ΦCO_2). Two-way ANOVA was used to test for the effects of photosynthetic pathway, oxygen concentration, and their interactions on steady state photosynthesis parameters; and three-way ANOVA to test for the effects of photosynthetic pathway, fluctuation length, oxygen concentration, and their interactions on A_{CO2} relative to steady state and ΦCO_2. Specifically for the ΦCO_2 analysis, the quantum yields obtained under steady state at 800 and 100 µmol m^{-2} s^{-1} PFD were included in the dataset as an additional fluctuation length. For each ANOVA, assumptions of normality, homogeneity of variance and sphericity were satisfied. Mean and standard error of the mean for steady state photosynthesis parameters, A_{CO2} relative to steady state, and ΦCO_2 across the light fluctuation regimes were calculated for reporting.

All data analysis and plot generation was done with R 4.1.1 (R Core Team, 2021) on RStudio 2022.12.0+353 (Posit Team, 2022) using the tidyverse (Wickham et al., 2019), RColorBrewer (Neuwirth, 2014), lme4 (Bates et al., 2015) , and bayestestR libraries (Makowski et al., 2019).

Acknowledgements
Lucía Arce Cubas was jointly funded by The Cambridge Commonwealth, European & International Trust; and by Mexico's Consejo Nacional de Ciencia y Tecnología (CONACyT). This work was supported by the BBSRC via grant BB/T007583/1 awarded to Dr. Johannes Kromdijk. The authors also thank Dr. Pascal-Antoine Christin at The University of Sheffield, Dr. Marjorie Lundgren at Lancaster Environmental Centre, and Prof. Peter Westhoff at Heinrich Heine University Düsseldorf for respectively providing the original *A. semialata GMT* and *MDG* accessions, *F. cronquistii* cuttings, and *F. bidentis* seeds. For the purpose of open access, the authors have applied a Creative Commons Attribution (CC BY) licence to any Author Accepted Manuscript version arising from this submission.

Author contributions
JK and LAC conceived the study. JK, LAC and ACB designed the experiments. LAC carried out all experiments, data analysis and interpretation, and drafted the manuscript. CRGS helped with the fluctuating light experimental setup and data interpretation. RLV helped with the 2% O_2 experimental setup and provided support with gas exchange experiments. ELB procured the initial plant material. All authors contributed to the article and approved the submitted version.

References

ACEVEDO-SIACA, L. G., COE, R., WANG, Y., KROMDIJK, J., QUICK, W. P. & LONG, S. P. 2020. Variation in photosynthetic induction between rice accessions and its potential for improving productivity. *New Phytologist,* 227**,** 1097-1108.

ARCE CUBAS, L., VATH, R. L., BERNARDO, E. L., SALES, C. R. G., BURNETT, A. C. & KROMDIJK, J. 2023. Activation of CO_2 assimilation during photosynthetic induction is slower in C_4 than in C_3 photosynthesis in three phylogenetically controlled experiments. *Frontiers in Plant Science,* 13.

ARRIVAULT, S., OBATA, T., SZECÓWKA, M., MENGIN, V., GUENTHER, M., HOEHNE, M., FERNIE, A. R. & STITT, M. 2017. Metabolite pools and carbon flow during C4 photosynthesis in maize: 13CO2 labeling kinetics and cell type fractionation. *Journal of Experimental Botany,* 68**,** 283-298.

BATES, D., MÄCHLER, M., BOLKER, B. & WALKER, S. 2015. Fitting Linear Mixed-Effects Models Using lme4. *Journal of Statistical Software,* 67**,** 1 - 48.

BELLASIO, C. & FARQUHAR, G. D. 2019. A leaf-level biochemical model simulating the introduction of C_2 and C_4 photosynthesis in C_3 rice: gains, losses and metabolite fluxes. *New Phytologist,* 223**,** 150-166.

BORGHI, G. L., ARRIVAULT, S., GÜNTHER, M., BARBOSA MEDEIROS, D., DELL'AVERSANA, E., FUSCO, G. M., CARILLO, P., LUDWIG, M., FERNIE, A. R., LUNN, J. E. & STITT, M. 2022. Metabolic profiles in C3, C3-C4 intermediate, C4-like, and C4 species in the genus Flaveria. *Journal of Experimental Botany,* 73**,** 1581-1601.

BRÄUTIGAM, A., HOFFMANN-BENNING, S. & WEBER, A. P. 2008. Comparative proteomics of chloroplast envelopes from C3 and C4 plants reveals specific adaptations of the plastid envelope to C4 photosynthesis and candidate proteins required for maintaining C4 metabolite fluxes. *Plant Physiol,* 148**,** 568-79.

CALSA, T. & FIGUEIRA, A. 2007. Serial analysis of gene expression in sugarcane (*Saccharum* spp.) leaves revealed alternative C4 metabolism and putative antisense transcripts. *Plant Molecular Biology,* 63**,** 745-762.

CHRISTIN, P.-A., OSBORNE, C. P., SAGE, R. F., ARAKAKI, M. & EDWARDS, E. J. 2011. C4 eudicots are not younger than C4 monocots. *Journal of Experimental Botany,* 62**,** 3171-3181.

EHLERINGER, J. & PEARCY, R. W. 1983. Variation in Quantum Yield for CO2 Uptake among C3 and C4 Plants. *Plant Physiology,* 73**,** 555-559.

FAO 2020. Production, Trade and Prices of Commodities. *World Food and Agriculture - Statistical Yearbook 2020.* Rome, Italy: FAO.

FORRESTER, M. L., KROTKOV, G. & NELSON, C. D. 1966. Effect of oxygen on photosynthesis, photorespiration and respiration in detached leaves. I. Soybean. *Plant Physiol,* 41**,** 422-7.

FURBANK, R. T. 2011. Evolution of the C4 photosynthetic mechanism: are there really three C4 acid decarboxylation types? *Journal of Experimental Botany,* 62**,** 3103-3108.

GOWIK, U., BRÄUTIGAM, A., WEBER, K. L., WEBER, A. P. M. & WESTHOFF, P. 2011. Evolution of C4 Photosynthesis in the Genus *Flaveria*: How Many and Which Genes Does It Take to Make C4? *The Plant Cell,* 23**,** 2087-2105.

GU, J., YIN, X., STOMPH, T.-J. & STRUIK, P. C. 2014. Can exploiting natural genetic variation in leaf photosynthesis contribute to increasing rice productivity? A simulation analysis. *Plant, Cell & Environment,* 37**,** 22-34.

HATCH, M., KAGAWA, T. & CRAIG, S. 1975. Subdivision of C4-Pathway Species Based on Differing C4 Acid Decarboxylating Systems and Ultrastructural Features. *Functional Plant Biology,* 2**,** 111-128.

ISHIKAWA, N., TAKABAYASHI, A., SATO, F. & ENDO, T. 2016. Accumulation of the components of cyclic electron flow around photosystem I in C_4 plants, with respect to the requirements for ATP. *Photosynthesis Research,* 129**,** 261-277.

JAWIEŃ, W. 2014. Searching for an optimal AUC estimation method: a never-ending task? *Journal of Pharmacokinetics and Pharmacodynamics,* 41**,** 655-673.

KAISER, E., MORALES, A. & HARBINSON, J. 2018. Fluctuating Light Takes Crop Photosynthesis on a Rollercoaster Ride. *Plant Physiology,* 176**,** 977-989.

KAISER, E., MORALES, A., HARBINSON, J., KROMDIJK, J., HEUVELINK, E. & MARCELIS, L. F. M. 2015. Dynamic photosynthesis in different environmental conditions. *Journal of Experimental Botany,* 66**,** 2415-2426.

KELLOGG, E. A. 2013. C4 photosynthesis. *Current Biology,* 23**,** R594-R599.

KINIRY, J. R., JONES, C. A., O'TOOLE, J. C., BLANCHET, R., CABELGUENNE, M. & SPANEL, D. A. 1989. Radiation-use efficiency in biomass accumulation prior to grain-filling for five grain-crop species. *Field Crops Research,* 20**,** 51-64.

KOK, B. 1949. On the interrelation of respiration and photosynthesis in green plants. *Biochimica et Biophysica Acta,* 3**,** 625-631.

KRALL, J. P. & PEARCY, R. W. 1993. Concurrent Measurements of Oxygen and Carbon Dioxide Exchange during Lightflecks in Maize (Zea mays L.). *Plant Physiology,* 103**,** 823-828.

KROMDIJK, J., GŁOWACKA, K., LEONELLI, L., GABILLY, S. T., IWAI, M., NIYOGI, K. K. & LONG, S. P. 2016. Improving photosynthesis and crop productivity by accelerating recovery from photoprotection. *Science,* 354**,** 857-861.

KROMDIJK, J., GRIFFITHS, H. & SCHEPERS, H. E. 2010. Can the progressive increase of C_4 bundle sheath leakiness at low PFD be explained by incomplete suppression of photorespiration? *Plant, Cell & Environment,* 33**,** 1935-48.

KROMDIJK, J., UBIERNA, N., COUSINS, A. B. & GRIFFITHS, H. 2014. Bundle-sheath leakiness in C4 photosynthesis: a careful balancing act between CO2 concentration and assimilation. *Journal of Experimental Botany,* 65**,** 3443-57.

KUBÁSEK, J., URBAN, O. & ŠANTRŮČEK, J. 2013. C4 plants use fluctuating light less efficiently than do C3 plants: a study of growth, photosynthesis and carbon isotope discrimination. *Physiologia Plantarum,* 149**,** 528-539.

LAISK, A. & EDWARDS, G. E. 1997. Post-illumination CO_2 Exchange and Light-induced CO_2 Bursts during C_4 Photosynthesis. *Functional Plant Biology,* 24**,** 517-528.

LAWSON, T., KRAMER, D. M. & RAINES, C. A. 2012. Improving yield by exploiting mechanisms underlying natural variation of photosynthesis. *Current Opinion in Biotechnology,* 23**,** 215-220.

LEE, M. S., BOYD, R. A. & ORT, D. R. 2022. The photosynthetic response of C3 and C4 bioenergy grass species to fluctuating light. *GCB Bioenergy,* 14**,** 37-53.

LEEGOOD, R. C. 2002. C4 photosynthesis: principles of CO2 concentration and prospects for its introduction into C3 plants. *Journal of Experimental Botany,* 53**,** 581-590.

LEEGOOD, R. C. & FURBANK, R. T. 1984. Carbon metabolism and gas exchange in leaves of *Zea mays* L. *Planta,* 162**,** 450-456.

LEEGOOD, R. C. & VON CAEMMERER, S. 1989. Some relationships between contents of photosynthetic intermediates and the rate of photosynthetic carbon assimilation in leaves of *Zea mays L. Planta,* 178**,** 258-266.

LI-COR, I. 1988. *1800-12 Integrating Sphere Instruction Manual.*

LI, Y.-T., LUO, J., LIU, P. & ZHANG, Z.-S. 2021. C4 species utilize fluctuating light less efficiently than C3 species. *Plant Physiology,* 187**,** 1288-1291.

LILLEY, R. M., CHON, C. J., MOSBACH, A. & HELDT, H. W. 1977. The distribution of metabolites between spinach chloroplasts and medium during photosynthesis in vitro. *Biochimica et Biophysica Acta (BBA) - Bioenergetics,* 460**,** 259-272.

LONG, S. P., ZHU, X.-G., NAIDU, S. L. & ORT, D. R. 2006. Can improvement in photosynthesis increase crop yields? *Plant, Cell and Environment,* 29**,** 315-330.

LUNDGREN, M. R., BESNARD, G., RIPLEY, B. S., LEHMANN, C. E. R., CHATELET, D. S., KYNAST, R. G., NAMAGANDA, M., VORONTSOVA, M. S., HALL, R. C., ELIA, J., OSBORNE, C. P. & CHRISTIN, P.-A. 2015. Photosynthetic innovation broadens the niche within a single species. *Ecology Letters,* 18**,** 1021-1029.

MAKOWSKI, D., BEN-SHACHAR, M. S. & LÜDECKE, D. 2019. bayestestR: Describing Effects and their Uncertainty, Existence and Significance within the Bayesian Framework. *Journal of Open Source Software,* 4**,** 1541.

MCAUSLAND, L., VIALET-CHABRAND, S., DAVEY, P., BAKER, N. R., BRENDEL, O. & LAWSON, T. 2016. Effects of kinetics of light-induced stomatal responses on photosynthesis and water-use efficiency. *New Phytologist,* 211**,** 1209-1220.

MEDEIROS, D. B., ISHIHARA, H., GUENTHER, M., ROSADO DE SOUZA, L., FERNIE, A. R., STITT, M. & ARRIVAULT, S. 2022. 13CO2 labeling kinetics in maize reveal impaired efficiency of C4 photosynthesis under low irradiance. *Plant Physiology,* 190**,** 280-304.

MORALES, A., KAISER, E., YIN, X., HARBINSON, J., MOLENAAR, J., DRIEVER, S. M. & STRUIK, P. C. 2018. Dynamic modelling of limitations on improving leaf CO2 assimilation under fluctuating irradiance. *Plant, Cell & Environment,* 41**,** 589-604.

MOTT, K. A. & WOODROW, I. E. 2000. Modelling the role of Rubisco activase in limiting non-steady-state photosynthesis. *Journal of Experimental Botany,* 51**,** 399-406.

NEUWIRTH, E. 2014. RColorBrewer: ColorBrewer Palettes.

NIU, Y., LAZÁR, D., HOLZWARTH, A. R., KRAMER, D. M., MATSUBARA, S., FIORANI, F., POORTER, H., SCHREY, S. D. & NEDBAL, L. 2022. A plant's capacity to cope with fluctuating light depends on the frequency characteristics of non-photochemical quenching and cyclic electron transport. Cold Spring Harbor Laboratory.

PEARCY, R. W. 1990. Sunflecks and Photosynthesis in Plant Canopies. *Annual Review of Plant Physiology and Plant Molecular Biology,* 41**,** 421-453.

PEARCY, R. W., GROSS, L. J. & HE, D. 1997. An improved dynamic model of photosynthesis for estimation of carbon gain in sunfleck light regimes. *Plant, Cell & Environment,* 20**,** 411-424.

PEARCY, R. W. & SEEMANN, J. R. 1990. Photosynthetic Induction State of Leaves in a Soybean Canopy in Relation to Light Regulation of Ribulose-1-5-Bisphosphate Carboxylase and Stomatal Conductance. *Plant Physiology,* 94**,** 628-633.

PICK, T. R., BRÄUTIGAM, A., SCHULZ, M. A., OBATA, T., FERNIE, A. R. & WEBER, A. P. M. 2013. *PLGG1*, a plastidic glycolate glycerate transporter, is required for photorespiration and defines a unique class of metabolite transporters. *Proceedings of the National Academy of Sciences,* 110**,** 3185-3190.

PIGNON, C. P., LEAKEY, A. D. B., LONG, S. P. & KROMDIJK, J. 2021. Drivers of Natural Variation in Water-Use Efficiency Under Fluctuating Light Are Promising Targets for Improvement in Sorghum. *Frontiers in Plant Science,* 12**,** 627432.

PONS, T. L. & PEARCY, R. W. 1992. Photosynthesis in flashing light in soybean leaves grown in different conditions. II. Lightfleck utilization efficiency. *Plant, Cell and Environment,* 15**,** 577-584.

POSIT TEAM 2022. RStudio: Integrated Development Environment for R. Boston, MA: Posit Software, PBC.

R CORE TEAM 2021. R: A Language and Environment for Statistical Computing. Vienna, Austria: R Foundation for Statistical Computing.

SAGE, R. F. 2000. C_3 versus C_4 photosynthesis in rice: ecophysiological perspectives. *In:* SHEEHY, J. E., MITCHELL, P. L. & HARDY, B. (eds.) *Studies in Plant Science.* Elsevier.

SAGE, R. F. 2004. The evolution of C4 photosynthesis. *New Phytologist,* 161**,** 341-370.

SAGE, R. F. & MCKOWN, A. D. 2006. Is C4 photosynthesis less phenotypically plastic than C3 photosynthesis? *Journal of Experimental Botany,* 57**,** 303-317.

SALES, C. R. G., RIBEIRO, R. V., HAYASHI, A. H., MARCHIORI, P. E. R., SILVA, K. I., MARTINS, M. O., SILVEIRA, J. A. G., SILVEIRA, N. M. & MACHADO, E. C. 2018. Flexibility of C4 decarboxylation and photosynthetic plasticity in sugarcane plants under shading. *Environmental and Experimental Botany,* 149**,** 34-42.

SALES, C. R. G., WANG, Y., EVERS, J. B. & KROMDIJK, J. 2021. Improving C4 photosynthesis to increase productivity under optimal and suboptimal conditions. *Journal of Experimental Botany,* 72**,** 5942-5960.

SASSENRATH-COLE, G. F. & PEARCY, R. W. 1992. The Role of Ribulose-1,5-Bisphosphate Regeneration in the Induction Requirement of Photosynthetic CO_2 Exchange under Transient Light Conditions. *Plant Physiology,* 99**,** 227-34.

SHARKEY, T. D., SEEMANN, J. R. & PEARCY, R. W. 1986. Contribution of Metabolites of Photosynthesis to Postillumination CO2 Assimilation in Response to Lightflects. *Plant Physiology,* 82**,** 1063-1068.

SLATTERY, R. A., WALKER, B. J., WEBER, A. P. M. & ORT, D. R. 2018. The Impacts of Fluctuating Light on Crop Performance. *Plant Physiology,* 176**,** 990-1003.

STITT, M., WIRTZ, W., GERHARDT, R., HELDT, H. W., SPENCER, C., WALKER, D. & FOYER, C. 1985. A comparative study of metabolite levels in plant leaf material in the dark. *Planta,* 166**,** 354-64.

STITT, M. & ZHU, X.-G. 2014. The large pools of metabolites involved in intercellular metabolite shuttles in C4 photosynthesis provide enormous flexibility and robustness in a fluctuating light environment. *Plant, Cell & Environment,* 37**,** 1985-1988.

TANG, Y.-H., WASHITANI, I., TSUCHIYA, T. & IWAKI, H. 1988. Fluctuation of photosynthetic photon flux density within a Miscanthus sinensis canopy. *Ecological Research,* 3**,** 253-266.

TAYLOR, S. H., HULME, S. P., REES, M., RIPLEY, B. S., IAN WOODWARD, F. & OSBORNE, C. P. 2010. Ecophysiological traits in C_3 and C_4 grasses: a phylogenetically controlled screening experiment. *New Phytologist,* 185**,** 780-791.

TAYLOR, S. H. & LONG, S. P. 2017. Slow induction of photosynthesis on shade to sun transitions in wheat may cost at least 21% of productivity. *Philosophical Transactions of the Royal Society B: Biological Sciences,* 372**,** 20160543.

UBIERNA, N., SUN, W. & COUSINS, A. B. 2011. The efficiency of C4 photosynthesis under low light conditions: assumptions and calculations with CO2 isotope discrimination. *Journal of Experimental Botany,* 62**,** 3119-3134.

UENO, O. & SENTOKU, N. 2006. Comparison of leaf structure and photosynthetic characteristics of C3 and C4 *Alloteropsis semialata* subspecies. *Plant, Cell & Environment,* 29**,** 257-268.

WANG, C., GUO, L., LI, Y. & WANG, Z. 2012. Systematic Comparison of C3 and C4 Plants Based on Metabolic Network Analysis. *BMC Systems Biology,* 6**,** S9.

WANG, Y., BRÄUTIGAM, A., WEBER, A. P. M. & ZHU, X.-G. 2014a. Three distinct biochemical subtypes of C4 photosynthesis? A modelling analysis. *Journal of Experimental Botany,* 65**,** 3567-3578.

WANG, Y., LONG, S. P. & ZHU, X. G. 2014b. Elements required for an efficient NADP-malic enzyme type C4 photosynthesis. *Plant Physiology,* 164**,** 2231-46.

WANG, Y., STUTZ, S. S., BERNACCHI, C. J., BOYD, R. A., ORT, D. R. & LONG, S. P. 2022. Increased bundle - sheath leakiness of CO2 during photosynthetic induction shows a lack of coordination between the C4 and C4 cycles. *New Phytologist,* 236**,** 1661-1675.

WAY, D. A. & PEARCY, R. W. 2012. Sunflecks in trees and forests: from photosynthetic physiology to global change biology. *Tree Physiology,* 32**,** 1066-1081.

WICKHAM, H., AVERICK, M., BRYAN, J., CHANG, W., MCGOWAN, L., FRANÇOIS, R., GROLEMUND, G., HAYES, A., HENRY, L., HESTER, J., KUHN, M., PEDERSEN, T., MILLER, E., BACHE, S., MÜLLER, K., OOMS, J., ROBINSON, D., SEIDEL, D., SPINU, V., TAKAHASHI, K., VAUGHAN, D., WILKE, C., WOO, K. & YUTANI, H. 2019. Welcome to the Tidyverse. *Journal of Open Source Software,* 4**,** 1686.

WYNN, T., BROWN, H., CAMPBELL, W. H. & BLACK, C. C., JR. 1973. Dark Release of $^{14}CO_2$ from Higher Plant Leaves. *Plant Physiology,* 52**,** 288-291.

YIN, X. & STRUIK, P. C. 2018. The energy budget in C4 photosynthesis: insights from a cell-type-specific electron transport model. *New Phytologist,* 218**,** 986-998.

YIN, X. & STRUIK, P. C. 2021. Exploiting differences in the energy budget among C_4 subtypes to improve crop productivity. *New Phytologist,* 229**,** 2400-2409.

YOSHIMURA, Y., KUBOTA, F. & UENO, O. 2004. Structural and biochemical bases of photorespiration in C4 plants: quantification of organelles and glycine decarboxylase. *Planta,* 220**,** 307-317.

ZHU, X. G., ORT, D. R., WHITMARSH, J. & LONG, S. P. 2004. The slow reversibility of photosystem II thermal energy dissipation on transfer from high to low light may cause large losses in carbon gain by crop canopies: a theoretical analysis. *J Exp Bot,* 55**,** 1167-75.

TABLES

Table 1: Photosynthetic parameters estimated from steady state light response curves under 21% and 2% O_2 on phylogenetically linked C_3 and C_4 *Alloteropsis*, *Flaveria* and *Cleome* species. Respiration in the light (*Rd*) was calculated by fitting the light response curves with a non-rectangular hyperbola. Values for *800* A_{CO2}, *100* A_{CO2}, $C_{i\ 800}$, $C_{i\ 100}$, *800* ΦCO_2, and *100* ΦCO_2 were taken at PFD = 800 µmol m^{-2} s^{-1} and PFD = 100 µmol m^{-2} s^{-1}. Means and standard error of the mean are shown (n = 5).

		21% Oxygen		**2% Oxygen**	
Genus	**Parameter**	**C_3**	**C_4**	**C_3**	**C_4**
Alloteropsis	*800* A_{CO2} (µmol m^{-2} s^{-1})	11.3 ± 0.9	12.3 ± 0.5	15.0 ± 1.2	13.1 ± 0.1
	100 A_{CO2} (µmol m^{-2} s^{-1})	3.2 ± 0.5	4.7 ± 0.5	4.8 ± 0.7	4.7 ± 0.7
	$C_{i\ 800}$ (µmol mol^{-1})	235 ± 20	265 ± 15	207 ± 21	245 ± 20
	$C_{i\ 100}$ (µmol mol^{-1})	348 ± 9	349 ± 2	334 ± 9	345 ± 2
	800 ΦCO_2	0.017 ± 0.003	0.021 ± 0.002	0.025 ± 0.006	0.022 ± 0.00
	100 ΦCO_2	0.047 ± 0.012	0.075 ± 0.014	0.065 ± 0.005	0.076 ± 0.018
	Rd	0.6 ± 0.1	1.7 ± 0.3	1.5 ± 0.3	1.5 ± 0.1
Flaveria	*800* A_{CO2} (µmol m^{-2} s^{-1})	13.8 ± 1.4	18.7 ± 1.0	25.0 ± 2.9	21.5 ± 1.7
	100 A_{CO2} (µmol m^{-2} s^{-1})	3.9 ± 0.2	4.2 ± 0.3	6.6 ± 0.3	4.7 ± 0.4
	$C_{i\ 800}$ (µmol mol^{-1})	246 ± 25	157 ± 8	230 ± 8	182 ± 18
	$C_{i\ 100}$ (µmol mol^{-1})	352 ± 6	339 ± 4	351 ± 5	343 ± 9
	800 ΦCO_2	0.022 ± 0.004	0.027 ± 0.00	0.038 ± 0.01	0.030 ± 0.005
	100 ΦCO_2	0.057 ± 0.005	0.057 ± 0.007	0.085 ± 0.01	0.056 ± 0.009
	Rd	0.4 ± 0.4	0.8 ± 0.3	0.6 ± 0.2	0.4 ± 0.2
Cleome	*800* A_{CO2} (µmol m^{-2} s^{-1})	14.6 ± 0.5	23.5 ± 2.0	27.3 ± 4.0	27.4 ± 0.9
	100 A_{CO2} (µmol m^{-2} s^{-1})	4.1 ± 0.2	3.2 ± 0.4	6.2 ± 0.6	4.7 ± 0.5
	$C_{i\ 800}$ (µmol mol^{-1})	281 ± 14	190 ± 12	266 ± 21	192 ± 9
	$C_{i\ 100}$ (µmol mol^{-1})	363 ± 7	352 ± 3	358 ± 18	344 ± 7
	800 ΦCO_2	0.020 ± 0.001	0.026 ± 0.006	0.033 ± 0.012	0.030 ± 0.003
	100 ΦCO_2	0.048 ± 0.004	0.056 ± 0.011	0.090 ± 0.016	0.061 ± 0.012
	Rd	1.5 ± 1.0	1.2 ± 0.4	2.1 ± 0.7	0.8 ± 0.5

Table 2: ANOVA table of light response curve parameters at 100 and 800 µmol m^{-2} s^{-1} PFD for phylogenetically linked C_3 and C_4 *Alloteropsis*, *Flaveria* and *Cleome* species. Photosynthetic pathway, PP. O_2 concentration, [O_2]. Interaction effect, PP:[O_2]. Table shows degrees of freedom; *F*-value; and *p*-value. Significant *p*-values ($a < 0.05$) are shown in bold.

	Alloteropsis			***Flaveria***			***Cleome***		
Parameter	**PP**	**[O_2]**	**PP:[O_2]**	**PP**	**[O_2]**	**PP:[O_2]**	**PP**	**[O_2]**	**PP:[O_2]**
800 A_{CO2}	1,16; 0.35; 0.56	1,16; 7.77; **0.01**	1,16; 3.24; 0.09	1,16; 0.12; 0.73	1,16; 13.48; **0.01**	1,16; 4.83; **0.04**	1,15; 0.01; 0.91	1,15; 6.18; **0.02**	1,15; 0.82; 0.28
100 A_{CO2}	1,16; 1.21; 0.29	1,16; 1.60; 0.22	1,16; 1.56; 0.23	1,16; 7.01; **0.02**	1,16; 25.64; **≤0.001**	1,16; 11.38; **0.01**	1,15; 7.28; **0.02**	1,15; 15,06; **0.01**	1,15; 0.43; 0.52
$C_{i\ 800}$	1,16; 3.21; 0.09	1,16; 1.62; 0.22	1,16; 0.05; 0.83	1,16; 17.63; **≤0.001**	1,16; 0.09; 0.76	1,16; 1.63; 0.22	1,16; 31.44; **≤0.001**	1,16; 0.19; 0.66	1,16; 1.33; 0.58
$C_{i\ 100}$	1,16; 0.87; 0.36	1,16; 1.96; 0.40	1,16; 0.74; 0.40	1,16; 2.52; 0.13	1,16; 0.11; 0.75	1,16; 0.16; 0.70	1,16; 3.65; 0.07	1,16; 1.01; 0.33	1,16; 0.04; 0.84
800 ΦCO_2	1,16; 0.22; 0.07	1,16; 8.12; **0.01**	1,16; 4.47; **0.05**	1,16; 0.13; 0.72	1,16; 11.90; **0.01**	1,16; 5.95; **0.03**	1,16; 0.19; 0.67	1,16; 6.96; **0.02**	1,16; 2.18; 0.15
100 ΦCO_2	1,16; 11.03; **0.01**	1,16; 2.67; 0.12	1,16; 2.04; 0.17	1,16; 15.56; **0.01**	1,16; 13.93; **0.01**	1,16; 16.53; **≤0.001**	1,16; 4.50; **0.05**	1,16; 21.01; **≤0.001**	1,16; 12.72; **0.01**

Table 3: ANOVA table of percentage A_{CO2} relative to steady state during the two different light steps of the light fluctuation treatments for phylogenetically linked C_3 and C_4 *Alloteropsis*, *Flaveria* and *Cleome* species. Photosynthetic pathway, PP. Fluctuating length, fl. O_2 concentration, [O_2]. Interaction effects, PP:fl, PP:[O_2], fl:[O_2], and PP:fl:[O_2]. Table shows degrees of freedom, *F*-value, and *p*-value. Significant *p*-values ($a < 0.05$) are shown in bold.

Light period (µmol m^{-2} s^{-1})	**Genus**	**PP**	**fl**	**[O_2]**	**PP:fl**	**PP:[O_2]**	**fl:[O_2]**	**PP:fl:[O_2]**
800	*Alloteropsis*	1,52; 0.01; 0.92	1,52; 3.64; 0.06	1,52; 0.01; 0.93	1,52; 0.96; 0.33	1,52; 0.13; 0.72	1,52; 0.19; 0.66	1,52; 0.00; 0.98
	Flaveria	1,52; 0.07; 0.80	1,52; 8.58; **0.01**	1,52; 13.90; **≤0.001**	1,52; 4.23; **0.04**	1,52; 4.65; **0.04**	1,52; 0.04; 0.84	1,52; 0.09; 0.76
	Cleome	1,52; 1.32; 0.25	1,52; 7.96; **0.01**	1,52; 0.53; 0.47	1,52; 0.00; 0.98	1,52; 1.54; 0.22	1,52; 0.72; 0.40	1,52; 0.00; 0.95
100	*Alloteropsis*	1,52; 1.15; 0.29	1,52; 15.30; **≤0.001**	1,52; 1.48; 0.23	1,52; 0.01; 0.90	1,52; 0.07; 0.79	1,52; 0.00; 0.96	1,52; 0.02; 0.89
	Flaveria	1,52; 14.20; **≤0.001**	1,52; 31.18; **≤0.001**	1,52; 0.50; 0.48	1,52; 0.94; 0.33	1,52; 0.03; 0.87	1,52; 0.24; 0.62	1,52; 0.02; 0.89
	Cleome	1,52; 7.65; **0.01**	1,52; 25.08; **≤0.001**	1,52; 0.50; 0.48	1,52; 2.64; 0.11	1,52; 3.06; 0.08	1,52; 0.00; 0.99	1,52; 0.53; 0.46

Table 4: ANOVA table of ΦCO_2 during the two different light steps of the light fluctuation treatments for phylogenetically linked C_3 and C_4 *Alloteropsis*, *Flaveria* and *Cleome* species. Photosynthetic pathway, PP. Fluctuating length, fl. O_2 concentration, $[O_2]$. Interaction effects, PP:fl, PP:$[O_2]$, fl:$[O_2]$, and PP:fl:$[O_2]$. Table shows degrees of freedom, *F*-value, and *p*-value. Significant *p*-values ($\alpha < 0.05$) are shown in bold.

Light period (μmol m^{-2} s^{-1})	**Genus**	**PP**	**fl**	**$[O_2]$**	**PP:fl**	**PP:$[O_2]$**	**fl:$[O_2]$**	**PP:fl:$[O_2]$**
800	*Alloteropsis*	1,52; 0.00; 0.97	1,52; 2.00; 0.16	1,52; 7.08; **0.01**	1,52; 0.76; 0.39	1,52; 1.22; 0.27	1,52; 0.20; 0.66	1,52; 0.00; 0.96
	Flaveria	1,52; 0.10; 0.75	1,52; 2.67; 0.11	1,52; 0.02; 0.89	1,52; 1.17; 0.28	1,52; 4.56; **0.03**	1,52; 0.40; 0.53	1,52; 0.77; 0.38
	Cleome	1,52; 0.01; 0.92	1,52; 11.15; **0.01**	1,52; 16.33; **≤0.001**	1,52; 0.53; 0.47	1,52; 4.45; **0.04**	1,52; 2.48; 0.12	1,52; 0.17; 0.68
100	*Alloteropsis*	1,52; 5.70; **0.02**	1,52; 23.37; **≤0.001**	1,52; 14.02; **≤0.001**	1,52; 0.25; 0.62	1,52; 0.94; 0.34	1,52; 0.04; 0.85	1,52; 0.07; 0.79
	Flaveria	1,52; 0.01; 0.94	1,52; 34.60; **≤0.001**	1,52; 1.28; 0.26	1,52; 0.00; 0.99	1,52; 3.26; 0.08	1,52; 1.15; 0.70	1,52; 0.17; 0.68
	Cleome	1,52; 1.04; 0.31	1,52; 38.70; **≤0.001**	1,52; 9.40; **0.02**	1,52; 1.21; **0.04**	1,52; 1.81; 0.28	1,52; 1.75; 0.19	1,52; 0.42; 0.52

Table 5: Phylogenetically linked C_3 and C_4 *Alloteropsis*, *Flaveria*, and *Cleome* species used in this study with their photosynthetic pathway, class, and main C_4 subtype if applicable.

Genus	**Species and accession**	**Photosynthetic pathway**	**C4 subtype**	**Class**
Alloteropsis	*Alloteropsis semialata* subspecies *semialata* accession GMT	C_3	---	Monocot
	Alloteropsis semialata subspecies *eckloniana* accession MDG	C_4	NADP-ME-PEPCK	
Flaveria	*Flaveria cronquistii*	C_3	---	Dicot
	Flaveria bidentis	C_4	NADP-ME	
Cleome	*Tarenaya hassleriana*	C_3	---	
	Gynandropsis gynandra	C_4	NAD-ME	

Figure legends

Figure 1: Light response curves of phylogenetically linked C_3 and C_4 *Alloteropsis*, *Flaveria* and *Cleome* species at 21% and 2% O_2. As a function of absorbed light intensity, plots show net CO_2 assimilation (A_{CO2}, **A, D**), intercellular CO_2 concentration (C_i, **B, E**), and stomatal conductance to water vapour (g_{sw}, **C, F**). Ribbons represent standard error of the mean (n=5).

Figure 2: Net CO_2 assimilation (A_{CO2}) in phylogenetically linked C_3 and C_4 *Alloteropsis*, *Flaveria* and *Cleome* species under three different fluctuating light regimes at 21% and 2% O_2. Each light regime consisted of alternating 800 and 100 µmol m^{-2} s^{-1} PFD periods, where each light step lasted 6, 30, or 300 seconds before changing. Treatments were started after leaves were acclimated at 150 µmol m^{-2} s^{-1} PFD and lasted 1 hour, data was analysed from minutes 50-60 of each treatment. Ribbons represent standard error of the mean (n=5). The full timeseries is shown in **Supplementary figure 1**.

Figure 3: Net CO_2 assimilation (A_{CO2}) relative to steady state (%) across the 800 and 100 µmol m^{-2} s^{-1} PFD light steps of differing length starting at the 50 minute mark, in white and grey respectively. Depending on the fluctuating light treatment, subplots are showing one complete fluctuation of 12, 60, or 600 seconds. Values represent A_{CO2} at a given point in the fluctuating light treatment relative to A_{CO2} obtained from steady state light response curves at the light intensity of each period in phylogenetically linked C_3 and C_4 *Alloteropsis*, *Flaveria* and *Cleome* species at 21% and 2% O_2. The dashed line represents 100%, where assimilation would be exactly that of steady state. Ribbons represent standard error of the mean (n=5). The corresponding absolute assimilation values are provided in **Supplementary figure 2**.

Figure 4: Boxplots of net CO_2 assimilation (A_{CO2}) relative to steady state (%) under the 800 and 100 µmol m^{-2} s^{-1} PFD light steps of the fluctuating light regimes. Each regime consisted of alternating 800 and 100 µmol m^{-2} s^{-1} PFD periods, where each light step lasted 6, 30, or 300 seconds. For each period, A_{CO2} across the timeseries for phylogenetically linked C_3 and C_4 *Alloteropsis*, *Flaveria* and *Cleome* species at 21% or 2% O_2 was calculated as a percentage of steady state values obtained from light response curves at the same light intensity and O_2 concentration. The dashed line represents 100%, where assimilation rate would equal steady state. Box edges represent the lower and upper quartiles, the solid line indicates the median, and points represent outliers beyond 1.5 times the interquartile range (n = 5 for each combination of species/oxygen). Three-way ANOVA (**Table 4**) was used to test the effect of photosynthetic pathway, fluctuating length, O_2 concentration and their interaction on A_{CO2}

relative to steady state in *Alloteropsis, Flaveria*, and *Cleome*. The corresponding absolute assimilation values are shown in **Supplementary figure 3.**

Figure 5: Boxplots of the quantum yield of carbon assimilation (ΦCO_2) under the 800 and 100 µmol m^{-2} s^{-1} PFD periods of the fluctuating light regimes or from steady state measurements. Each fluctuating regime consisted of alternating 800 and 100 µmol m^{-2} s^{-1} PFD periods, where each light step lasted 6, 30, or 300 seconds. Box edges represent the lower and upper quartiles, the solid line indicates the median, and points represent outliers beyond 1.5 times the interquartile range (n = 5 for each combination of species/measurement condition). Three-way ANOVA was used to test the effect of photosynthetic pathway, fluctuating length, O_2 concentration and their interaction on ΦCO_2 in *Alloteropsis, Flaveria*, and *Cleome* (results shown in **Table 5**).

Figures

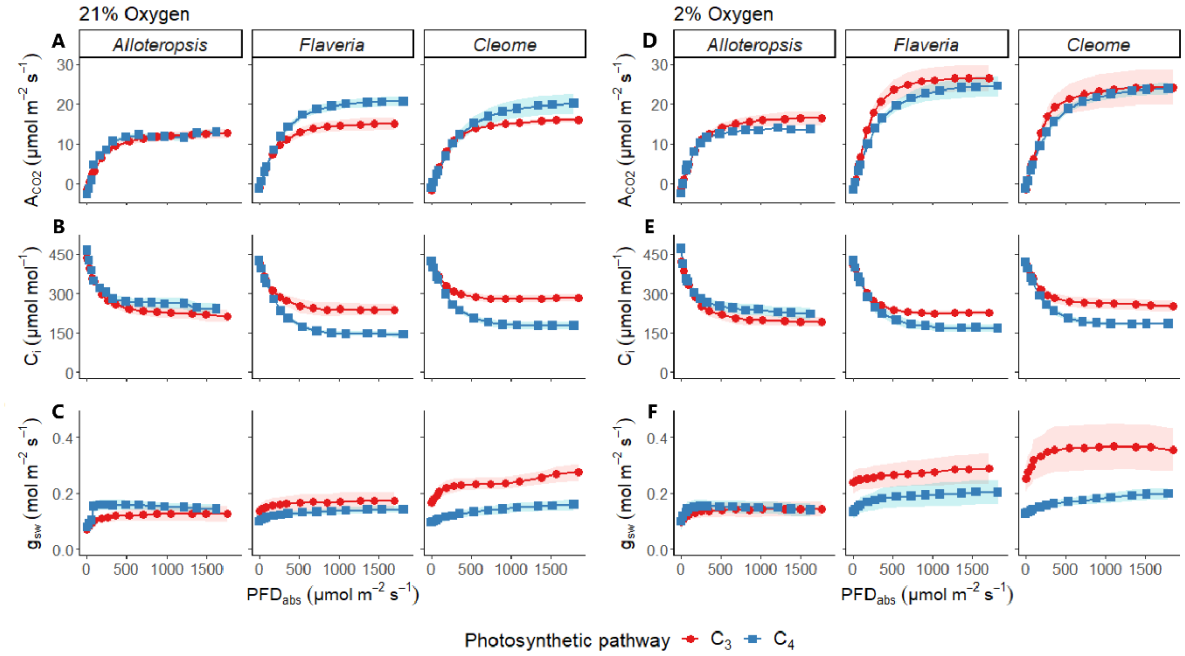

Figure 1: Light response curves of phylogenetically linked C_3 and C_4 *Alloteropsis*, *Flaveria* and *Cleome* species at 21% and 2% O_2. As a function of absorbed light intensity, plots show net CO_2 assimilation (A_{CO2}, **A, D**), intercellular CO_2 concentration (C_i, **B, E**), and stomatal conductance to water vapour (g_{sw}, **C, F**). Ribbons represent standard error of the mean (n=5).

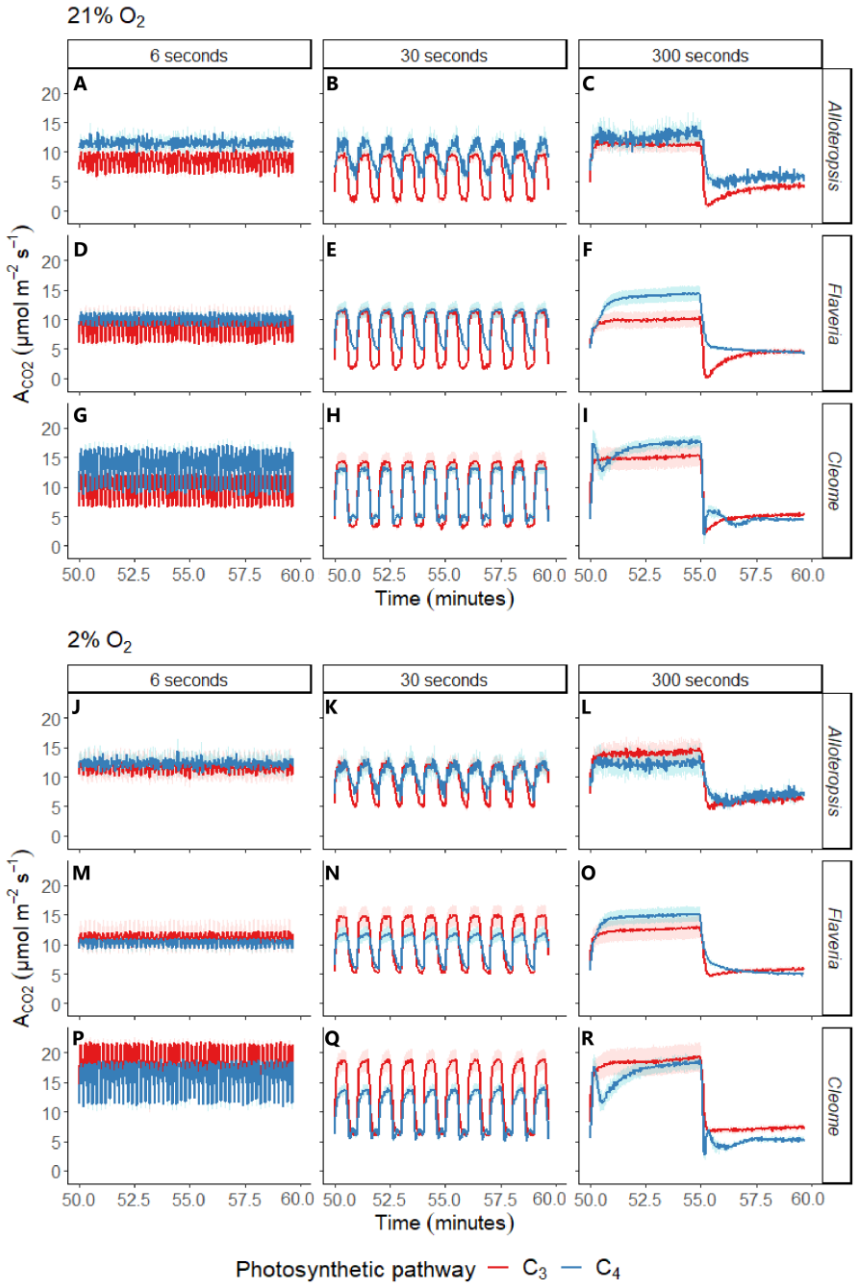

Figure 2: Net CO_2 assimilation (A_{CO2}) in phylogenetically linked C_3 and C_4 *Alloteropsis*, *Flaveria* and *Cleome* species under three different fluctuating light regimes at 21% and 2% O_2. Each light regime consisted of alternating 800 and 100 µmol m^{-2} s^{-1} PFD periods, where each light step lasted 6, 30, or 300 seconds before changing. Treatments were started after leaves were acclimated at 150 µmol m^{-2} s^{-1} PFD and lasted 1 hour, data was analysed from minutes 50-60 of each treatment. Ribbons represent standard error of the mean (n=5). The full timeseries is shown in **Supplementary figure 1**.

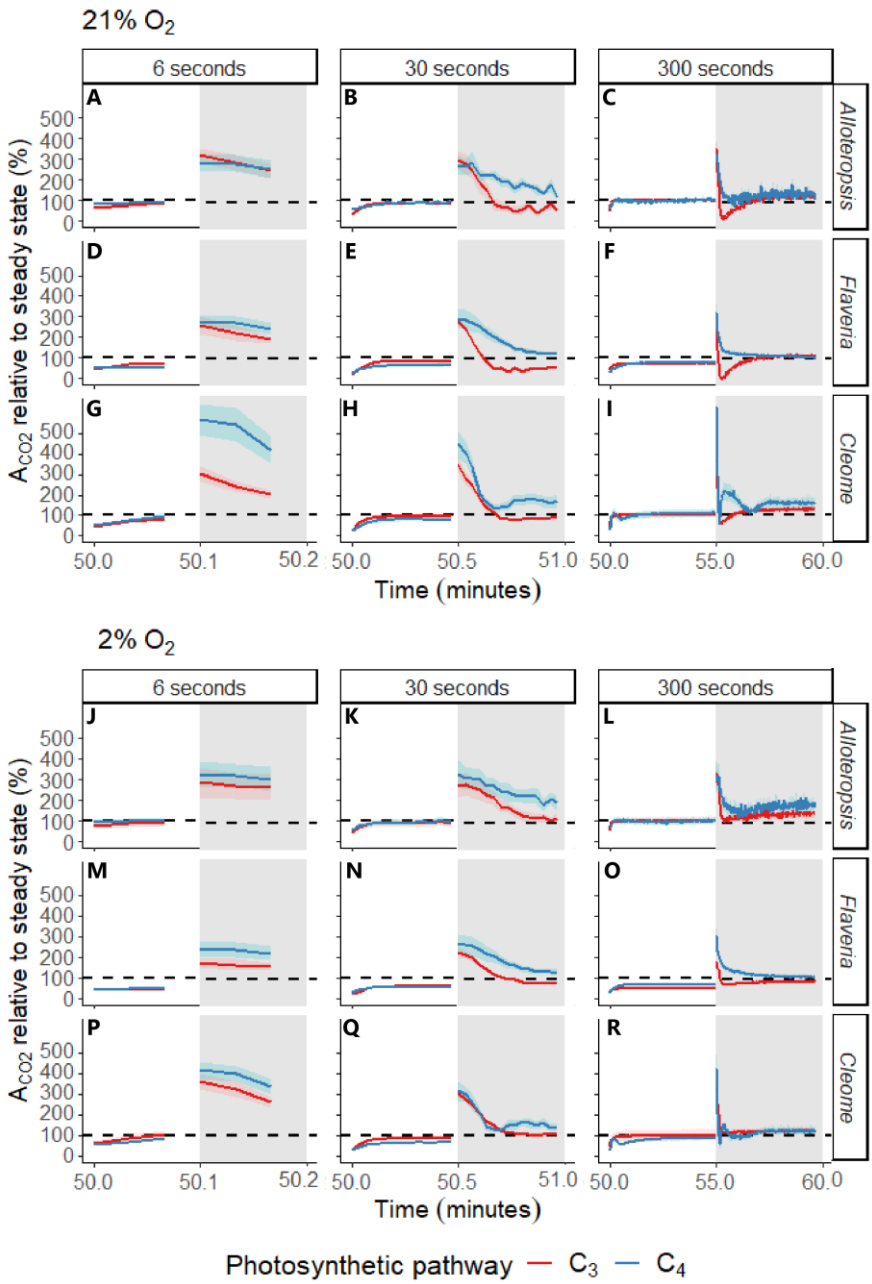

Figure 3: Net CO_2 assimilation (A_{CO2}) relative to steady state (%) across the 800 and 100 µmol m^{-2} s^{-1} PFD light steps of differing length starting at the 50 minute mark, in white and grey respectively. Depending on the fluctuating light treatment, subplots are showing one complete fluctuation of 12, 60, or 600 seconds. Values represent A_{CO2} at a given point in the fluctuating light treatment relative to A_{CO2} obtained from steady state light response curves at the light intensity of each period in phylogenetically linked C_3 and C_4 *Alloteropsis*, *Flaveria* and *Cleome* species at 21% and 2% O_2. The dashed line represents 100%, where assimilation would be exactly that of steady state. Ribbons represent standard error of the mean (n=5). The corresponding absolute assimilation values are provided in **Supplementary figure 2**.

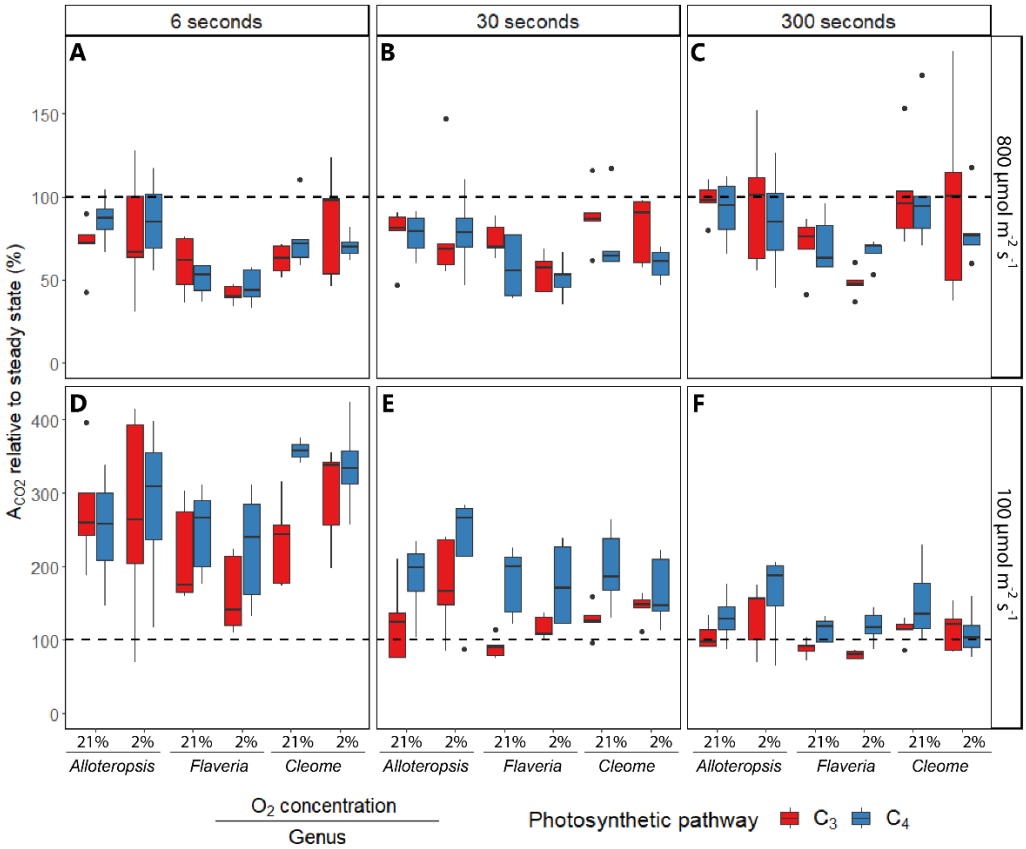

Figure 4: Boxplots of net CO_2 assimilation (A_{CO2}) relative to steady state (%) under the 800 and 100 µmol m^{-2} s^{-1} PFD light steps of the fluctuating light regimes. Each regime consisted of alternating 800 and 100 µmol m^{-2} s^{-1} PFD periods, where each light step lasted 6, 30, or 300 seconds. For each period, A_{CO2} across the timeseries for phylogenetically linked C_3 and C_4 *Alloteropsis*, *Flaveria* and *Cleome* species at 21% or 2% O_2 was calculated as a percentage of steady state values obtained from light response curves at the same light intensity and O_2 concentration. The dashed line represents 100%, where assimilation rate would equal steady state. Box edges represent the lower and upper quartiles, the solid line indicates the median, and points represent outliers beyond 1.5 times the interquartile range (n = 5 for each combination of species/oxygen). Three-way ANOVA (**Table 4**) was used to test the effect of photosynthetic pathway, fluctuating length, O_2 concentration and their interaction on A_{CO2} relative to steady state in *Alloteropsis, Flaveria*, and *Cleome*. The corresponding absolute assimilation values are shown in **Supplementary figure 3.**

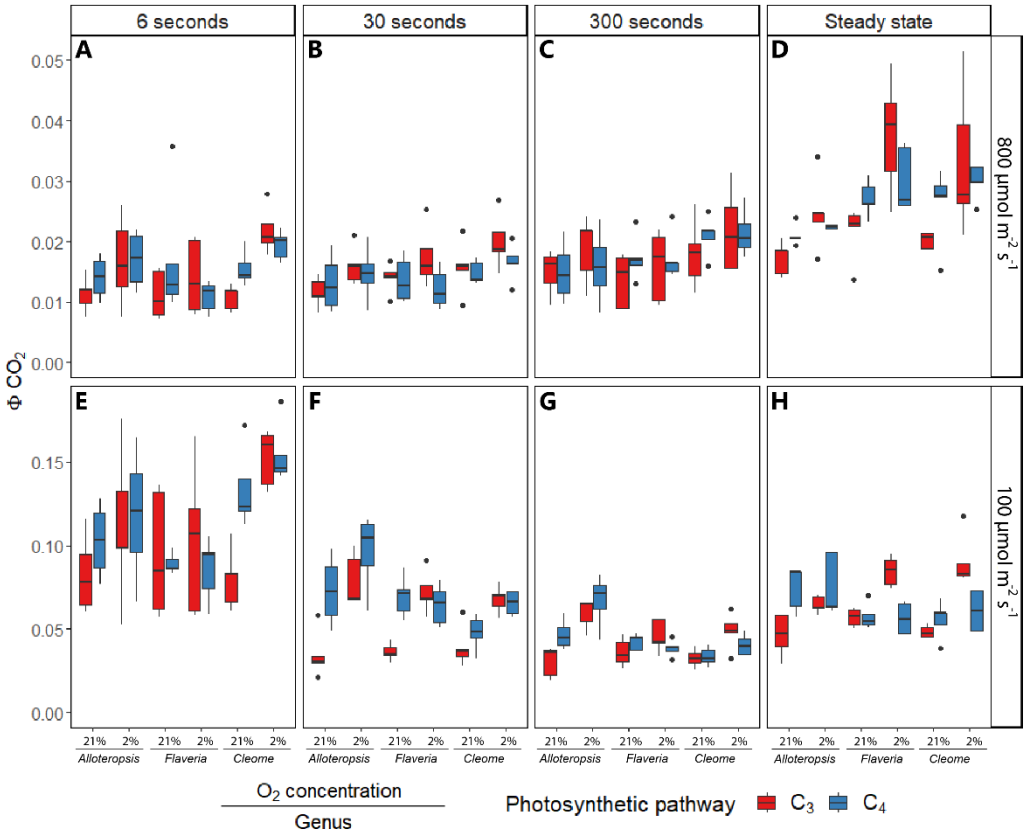

Figure 5: Boxplots of the quantum yield of carbon assimilation (ΦCO_2) under the 800 and 100 µmol m^{-2} s^{-1} PFD periods of the fluctuating light regimes or from steady state measurements. Each fluctuating regime consisted of alternating 800 and 100 µmol m^{-2} s^{-1} PFD periods, where each light step lasted 6, 30, or 300 seconds. Box edges represent the lower and upper quartiles, the solid line indicates the median, and points represent outliers beyond 1.5 times the interquartile range (n = 5 for each combination of species/measurement condition). Three-way ANOVA was used to test the effect of photosynthetic pathway, fluctuating length, O_2 concentration and their interaction on ΦCO_2 in *Alloteropsis, Flaveria*, and *Cleome* (results shown in **Table 5**).